Specialized Predation Drives Aberrant Morphological Integration and Diversity in the Earliest Ants

Phillip Barden, Vincent Perrichot, Bo Wang

Specialized predation drives aberrant morphological integration and diversity in the earliest ants

Phillip Barden[a,b,*], Vincent Perrichot[c,*], and Bo Wang[d*]

[a]New Jersey Institute of Technology, Department of Biological Sciences, Dr Martin Luther King Jr Blvd, Newark, NJ 07102, USA.

[b]American Museum of Natural History, Division of Invertebrate Zoology, Central Park West, New York, NY 10024, USA.

[c]Univ Rennes, CNRS, Géosciences Rennes - UMR 6118, F-35000 Rennes, France.

[d] State Key Laboratory of Palaeobiology and Stratigraphy, Nanjing Institute of Geology and Palaeontology and Center for Excellence in Life and Paleoenvironment, Chinese Academy of Sciences, 39 East Beijing Road, Nanjing 210008, China.

[*]Correspondence to: barden@njit.edu, vincent.perrichot@univ-rennes1.fr, bowang@nigpas.ac.cn.

Lead contact: Phillip Barden (barden@njit.edu)

Summary

Extinct haidomyrmecine 'hell ants' are among the earliest ants known [1, 2]. These eusocial Cretaceous taxa diverged from extant lineages prior to the most recent common ancestor of all living ants [3] and possessed bizarre scythe-like mouthparts along with a striking array of horn-like cephalic projections [4, 5, 6]. Despite the morphological breadth of the fifteen thousand known extant ant species, phenotypic syndromes found in the Cretaceous are without parallel and the evolutionary drivers of extinct diversity are unknown. Here we provide a mechanistic explanation for aberrant hell ant morphology through phylogenetic reconstruction and comparative methods, as well as a newly reported specimen. We report a remarkable instance of fossilized predation that provides direct evidence for the function of dorsoventrally-expanded mandibles and elaborate horns. Our findings confirm the hypothesis that hell ants captured other arthropods between mandible and horn in a manner that could only be achieved by articulating their mouthparts in an axial plane perpendicular to that of modern ants. We demonstrate that the head capsule and mandibles of haidomyrmecines are uniquely integrated as a consequence of this predatory mode and covary across species while finding no evidence of such modular integration in extant ant groups. We suggest that hell ant cephalic integration – analogous to the vertebrate skull – triggered a pathway for an ancient adaptive radiation and expansion into morphospace unoccupied by any living taxon.

Results and Discussion

Extinct diversity is a hallmark of certain lineages but conspicuous only with sufficient fossil evidence. Even among the nine thousand extant species of birds, there are no hints of an ancient array of predatory theropods. Comparisons of marine penguins, flightless ratites, hummingbirds, and albatrosses will not yield reconstructions of ornamented spinosaurids or massive tyrannosaurs. New evidence reveals the same is true for ants. With over 15,500 species and subspecies across all post-producer trophic levels and nearly every terrestrial environment [7], modern ants are morphologically diverse [8]. Intraspecific caste specialization amplifies diversity in many species as worker form matches specialized function [9, 10], from foraging and food processing to defense and brood care. In effect there are tens of thousands of ant morphotypes [11]. Even as extant ants represent a remarkable assemblage of adaptive diversity, the boundaries of Recent morphology do not encompass the former expanses of early ants.

The ant fossil record begins with contemporaneous Burmese and Charentese ambers from France and Myanmar dated to the Albian-Cenomanian boundary (~100-99 Ma) [1, 2]. Over 50 ant species are known from the Cretaceous – of these, only two are definitively attributable to modern lineages. Most Cretaceous ants belong to extinct stem-group lineages [3]. While the first discovered Mesozoic ants were generalized anatomical composites of living ants and solitary aculeate wasps [12, 13], subsequent discoveries demonstrate the diversity of extinct ant lineages [1, 14, 15, 16, 17]. The most extreme examples are haidomyrmecine 'hell ants.' Defined by dorsoventrally expanded scythe-like mandibles, these taxa are present in Burmese and Charentese ambers, as well as Campanian-aged (~78 Ma) Canadian amber [18], but do not persist into the Cenozoic [3]. Underscoring their bizarre mouthparts are a variety of horn-like

cephalic appendages [4, 5, 6, 19]. The varied mandibles and horns of hell ants have no modern analog.

Initial phenotypic "explorations" have long been proposed as features of lineage history [20, 21]. Early adaptive radiations may give rise to a multitude of morphological innovations, with only a subset of phenotypes persisting into the present [22, 23, 24]. Modern ant morphology operates within the confines of a core set of structural elaborations that relate to niche occupation [25]: spines appear within lineages as cuticular extensions of existing modular elements and relate to defense as well as muscle attachment [26]; setae, ancestrally derived from marine crustaceans, are modified for sense, adhesion, and defense [27, 28]; head capsules and cuticle are broadened and flattened, rendering worker ants into living doors or gliders [8, 29]. Because they dictate many interactions with the environment, ant mandibles are frequently modified for prey capture or task performance through modifications in teeth or margins [30]. Across lineages, specialized mandibles may facilitate the shearing of vegetation [8], the capture or killing of other ant hosts in social parasites [31], or the removal of defensive adaptations in prey [32]. Even with these varied uses, the axis of mandibular movement within modern ants is essentially fixed – extant ant mandibles open in a primarily lateral plane [33]. Although unconfirmed until now by direct evidence, hell ant mandibles are suspected to have articulated in an axis perpendicular to that of living species, acting as a trap-jaw mechanism for prey capture [34]. Indirect evidence for this movement includes the presence of hypothesized sensory setae in the path of mandible closure [18, 34]; covariation between elongate mandibles and clypeal projections, which have been proposed to function together [4]; and the reinforcement of cuticle in the region where the mandibles would come into contact with the head capsule [5]. Here, we place haidomyrmecines in an expanded phylogenetic context, demonstrate their unique morphospace occupation linked to evolutionary integration, and report preserved predatory behavior to explain the extinct stem diversity of ants. Our results suggest that an early radiation into disparate morphospace was triggered by an innovation in mouthpart movement for specialized predation. This generated a pathway for phenotypic integration between mandible and head capsule, analogous to the vertebrate skull.

Phylogenetic analysis and comparative morphospace

Our Bayesian and parsimony optimizations of 65 characters across 46 taxa confirm all haidomyrmecine genera as a monophyletic stem group outside of modern ant lineages, potentially sister to all other ants [3] (Haidomyrmecinae [6]). We recover two reciprocally monophyletic hell ant groups, suggesting one origin of horns but two independent derivations of elongate horns (Figure 1). Horns are derived from extensions of the clypeus, a segment of the head capsule that is typically flattened and strictly anteriorly positioned in ants and other aculeates. The clade comprising *Aquilomyrmex*, *Dhagnathos*, and *Chonidris* has a medially raised anterior clypeal margin developed into a furrowed appendage that points anteriad. The remaining hell ant taxa have a posteriorly-derived clypeal projection resulting from an increase in cuticular elevation and accompanied by a second projection, the frontal triangle. In *Linguamyrmex* and *Ceratomyrmex*, the frontal triangle is fused to the clypeal projection. In taxa where it is not fused to the clypeal projection, such as *Haidomyrmex* and *Protoceratomyrmex*, the function of the frontal triangle is unknown; it may aid in muscular attachment [33]. Scythe-

like mandibles and clypeal modifications are synapomorphies for hell ants and represent a ground-plan for the last common ancestor of the lineage. Our comparisons of extant and Cretaceous morphospace consistently recover haidomyrmecines as distinct from other stem and crown ants, even as cephalic morphospace overlaps among other stem ants and living taxa (Figures 2A and S1B). We assessed evolutionary correlation between the clypeus and mandibles in a phylogenetic framework through Bayesian MCMC estimation and regression analyses of phylogenetic independent contrasts. Analyses of subsampled measurements from 112 extant and fossil species indicate that the variation in clypeal and mandibular size is uniquely coupled in hell ants, relative to modern ant lineages (Figures 2B and 2C).

Direct evidence of hell ant predation

Specimen NIGP163569 (Figures 3A-D) preserves an instance of haidomyrmecine prey capture in 98.79 ± 0.62 Ma Burmese amber [35]. A single worker of *Ceratomyrmex ellenbergeri* (Figure 1D) – a species of hell ant possessing enormous slender mandibles and horn – is restraining a *Caputoraptor elegans* nymph. *Caputoraptor* is known exclusively from Cretaceous Burmese amber and a member of the extinct dictyopteran order †Alienoptera (†Alienopteridae) [36, 37]. The mandibles and elongate horn of *C. ellenbergeri* are grasping the narrowed pronotal neck of the nymphal *C. elegans*, acting as a collar, a position which is only possible through vertical movement of the mandibles. *Caputoraptor* possesses an unusual cephalo-pronotal scissor-device, which has been hypothesized to aid in copulation, prey capture, or defense [37, 38]. Given the highly specific capture mode reported here, a rapid contraction of the head capsule against the serrated thorax by *Caputoraptor* may have been enough to evade predation by hell ants. Ants and almost all other hexapods have dicondylic mandibles, which limit movement to one axis. It is not yet known if hell ants have lost a condyle or restructured condyle placement, however extant ants notably exhibit modified mandible joints – the dorsal mandibular socket is widened and allows for gliding relative to the more restrictive ball-in-socket joint found in other Hymenoptera [39]. This gliding likely increases range of motion and could be implicated in hell ant prey capture.

Diversity in hell ant mandibles and horns likely reflects alternative adaptations for prey capture. Prey were either pinned or pierced between sharp mandibles and head appendages, which would kill on contact or allow for a subsequent immobilizing sting. Taxa with unarmed, elongate horns such as *Ceratomyrmex* apparently grasped prey externally. Others such as *Haidomyrmex* and *Linguamyrmex* are suspected to have impaled prey – potentially feeding on internal liquid released after mandibular strikes as in some extant trap jaw ants [5, 40].

A doomed Cretaceous radiation

Haidomyrmecine “hell ants” were undoubtedly predators. While the postcephalic features of the subfamily are consistent with other ant taxa [1, 14, 34], extreme modifications in cephalic morphology define this enigmatic group. Hell ant mandibles, typified by dorsal expansions and a sharp apical point, are expanded toward the vertex of the head [2, 4] while the clypeus is heavily modified into a variety of nodes and horns in the context of the mandibles (Figures 1A-G and S3). The apex of the mandibles and terminus of the clypeal processes are always in close proximity when mandibles are closed suggesting the two are functionally integrated [4, 18, 34].

In at least one haidomyrmecine, *Linguamyrmex vladi*, the clypeal horn cuticle appears to be medially reinforced, potentially with sequestered metals [5]. Accommodating the horn and mandible, the head is dorso-ventrally elongate in most haidomyrmecines, whereby the oral opening faces downward. While not hypognathous in the strict sense, this orientation is similar to that of other aculeate Hymenoptera and many insects [41]. Modern ants are prognathic [42], orienting their mouth forward by keeping the underside of the head parallel with the ground, although the head may be pulled back to nearly flush with the propleuron. Hell ants appear to have had limited head mobility and likely captured prey while keeping the oral opening downward, which positioned the mandibles forward while hunting.

Extant “trap-jaw” ants provide insight into prey capture in haidomyrmecines. Trap jaw syndromes – with rapidly closing mandibles that are released by a locking apparatus – have evolved at least four times in extant ants [43]. Trap-jaw ants lock their mandibles into a wide-open horizontal position until prey initiate power-amplified closure by stimulating specialized setae, or trigger hairs [44]. Rapidly closing mandibles strike prey, initially killing in some species or grasping until a venomous sting is applied [45]. These mandible strikes are among the fastest animal movements recorded [46]. Most haidomyrmecines have long, fine setae within the hypothesized range of mandibular movement that have been interpreted as trigger hairs (Figures 1A-D) [4, 5, 18, 34]. Some trap-jaw ants feed on fast moving prey such as springtails, but many are generalists, feeding on termites, orthopterans, and spiders [40, 47]. Extant trap-jaw ant mandibles do not make contact with the head capsule but close against each other and so mouthpart specialization reflects mandible-on-mandible contact (Figure 1J).

The Cretaceous ant fauna was rich, composed almost entirely of now extinct lineages that did not persist beyond the K–Pg boundary [3]. Molecular divergence date estimates indicate that crown ants extend into the Early Cretaceous [48, 49, 50, 51]. Early members of extant ant lineages coexisted with stem taxa, including hell ants, for tens of millions of years. Following their divergence in the Cretaceous, crown ants continued to diversify, with highest rates from the late Cretaceous through the Oligocene [49, 52]. Despite consistent increases in diversity over time among extant lineages [53], there has been no repeated evolution of haidomyrmecine-like morphology. Early expansions in morphological variation are well known in certain extinct taxa [54] but may be uncommon or difficult to measure [55, 56]. The evolutionary pathway for early diversity may also be ambiguous. Hell ants reflect a series of adaptive forms and a pattern of morphological diversity contingent on an innovation in mouthpart movement. Without an initial switch to vertically articulating mandibles, modern ant lineages never infiltrated the morphospace of their extinct counterparts.

Vertical mandible movement is present in aquatic larvae of some *Hydrophus* beetles [57, 58]. The larvae are predators of shelled shrimp, and use their specialized head projection in conjunction with mandibles to grasp prey [59]. Despite staggering anatomical diversity of insects, larval dytiscid beetles and hell ants together appear to represent the only two known instances of mandible-on-head contact used in prey capture [59], both appearing with vertically-articulating mouthparts. In the absence of a mandibular counterforce, mandibles interact with the head capsule [59] and act as a lower jaw analogous to the dentary and cranium of

vertebrates. An initial innovation in mandible articulation led to functional and evolutionary integration [60] and feedback between horn and mandible, which provided access to new adaptive space. The modular elements implicated in this syndrome were driven to striking extremes. Such a pattern is visible when comparing *Protoceratomyrmex*, with a weakly developed horn and stout mandibles, with *Linguamyrmex* and *Certomyrmex*, which possesses increasingly co-exaggerated features (Figures 1A-G and S3). A similar, convergent pattern is also present in a sister clade including *Dhagnathos* and *Ceratomyrmex* (Figures 1E-F).

The ecological pressures and developmental requirements that led to vertical mandible articulation are not yet known. Also unclear are the conditions that drove haidomyrmecines to extinction after persisting for a period of at least 20 million years across present day Asia, Europe, and North America. Predatory specialization may have rendered hell ants susceptible to extinction during periods of ecological change. However, generalized stem-group taxa – such as *Gerontoformica* – also disappear from the fossil record toward the end of the Cretaceous, suggesting other factors may have played a role including competition with burgeoning extant ants. While haidomyrmecines and other stem ants were eusocial – evidenced by distinct reproductive castes [2] – perhaps a distinct feature of crown ant sociality provided a bulwark against extinction. Regardless of the conditions leading to their loss, our findings implicate functional integration in shaping the aberrant phenotypic diversity of extinct taxa. Remarkably, this example came as an antecedent to one of the most ubiquitous terrestrial lineages alive today.

Acknowledgements

We are grateful to Martina Decker, Oliver Budd, Jackson Fordham, and Victor Nzegwu at the New Jersey Institute of Technology (NIJT) for 3D model reconstruction; Dinghua Yang (NIGPAS) for artistic reconstruction of predation; C. Sosiak (NIJT) with coding information for *Haidoterminus*; Peta Hayes and Claire Mellish for facilitating access to the Natural History Museum, London type material for P.B; D.A. Grimaldi, E.O. Wilson, and three anonymous reviewers provided helpful feedback that improved the manuscript. This research was supported by the Strategic Priority Research Program of the Chinese Academy of Sciences (XDB26000000) and National Natural Science Foundation of China (41688103).

Author Contributions

Conceptualization, P.B., V.P., and B.W.; Formal Analysis, P.B., and V.P.; Investigation, P.B., V.P., and B.W.; Methodology, P.B., V.P., and B.W.; Resources, P.B., V.P., and B.W.; Writing P.B., V.P., and B.W.

Declaration of Interests

The authors declare no competing interests.

Figure Legends

Fig. 1. Phylogeny and cephalic homology of hell ants and modern lineages. (Left) Relationships among ant lineages and stem ants from Bayesian optimization of 64 characters with constrained extant topology and divergence dates from Borowiec et al. [51]. (Right) Digitally sculpted 3D reconstructions of hell ant genera: (A) *Haidomyrmex*; (B) *Protoceratomyrmex*; (C) *Linguamyrmex*; (D) *Ceratomyrmex*; (E) *Dhagnathos*; (F) *Chonidris*; (G) *Aquilomyrmex*. Scanning electron microscopy micrographs of extant ants: (H) *Leptanilla*; (I) *Amblyopone*; (J) *Anochetus*; (K) *Aneuretus*; (L) *Nothomyrmecia*; (M) *Tetraponera*. H-I,K-M courtesy Roberto A. Keller/AMNH; J from Alex Wild. Orange: mandibles; Blue: clypeus; Yellow: labrum; Purple: frontal triangle. See also Figures S1 and S3, Table S1.

Fig. 2. Morphospace and evolutionary integration of living and Cretaceous ants. (A) Principal coordinate analysis morphospace of cephalic characters (variance: PCo1 30%, PCo2 19%). (B) Slope (inset) and R-squared summary of linear regression analyses. Regressions were performed on phylogenetic independent contrasts of scaled clypeal and mandibular area (maximum length x maximum height / head area) in lateral view. Each slope represents one of five subfamilial (n=8-15), three congeneric (n=9), or two Formicidae-wide (n=24, 61) subsamples. Hell ants exhibit a strong positive relationship and high coefficient of determination between these traits (m=1.3, R2 =0.93, P<0.001), a result of integration following an innovation in mandibular function. (C) Posterior distribution of Bayesian estimates of evolutionary correlation between clypeal and mandibular area in extant (n=24, $\bar{x}$ =0.18) and hell ant (n=8, $\bar{x}$ =0.72) taxa included in Fig. 1 phylogeny. See also Figures S1 and S2, Table S2.

Fig. 3. Predation preserved in amber. (A–C), specimen NIGP163569, a worker of *Ceratomyrmex ellenbergeri* grasping a nymph of *Caputoraptor elegans* (Alienoptera) preserved in Burmese amber dated to ~99 Ma. (A) dorsal view; (B) reconstruction of specimen; (C) ventral view of mandibles closed around the pronotal neck; (D) simplified reconstruction from oblique lateral view. Abbreviations: amd, apical portion of *Ceratomyrmex* mandibles; mib, mandibular medioventral blade of *Ceratomyrmex*; e, compound eye of *Caputoraptor*; pg, protruding extension of *Caputoraptor*'s gena.

STAR Methods

RESOURCE AVAILABILITY

Lead Contact

Further information and requests for resources and reagents should be directed to and will be fulfilled by the Lead Contact, Phillip Barden (barden@njit.edu).

Materials Availability

This study did not generate new unique reagents.

Data and Code Availability

The phylogenetic matrix and trees generated during this study are available at TreeBase [TB2:S26540]. The published article includes all morphometric data generated and analyzed during this study.

EXPERIMENTAL MODEL AND SUBJECT DETAILS

Studied material for reported predation

Specimen *NIGP163569*. A worker of *Ceratomyrmex ellenbergeri*, exposed in dorsal and ventral views, with an insect nymph (family †Alienopteridae) caught between the mandibles and the cephalic horn. The preservation is average, both syninclusions are coated in small bubbles attached to their exoskeleton. In a rounded piece of clear yellow amber measuring 13×10×6 mm. Note: The specimen – from the Hukawng Valley, Kachin State, Myanmar – was deposited in the Nanjing Institute of Geology and Palaeontology, Chinese Academy of Sciences (NIGPAS) prior to the 2017 military control of some mine regions (work on this manuscript began in early 2017). The fossil acquired by NIGPAS was collected in full compliance with the laws of Myanmar and China including Regulation on the Protection of Fossils of China. To avoid any confusion and misunderstanding, all authors declare that the fossil reported in this study was not involved in armed conflict and ethnic strife in Myanmar. The specimen is deposited in the public repository NIGPAS and is available for study.

Specimens for phylogenetic and morphometric data

All sampled specimens were adult female ants in museum collections. Specimens analyzed for phylogenetic coding and morphometric data collection are noted by specimen number in Data S1. All fossil specimens were previously described and are housed in the following collections: American Museum of Natural History (AMNH), Geology Department and Museum of the University Rennes 1 (IGR), Nanjing Institute of Geology and Palaeontology, Chinese Academy of Sciences (NIGPAS), and University of Alberta Strickland Entomology Museum (UASM). Morphometric measurements of extant taxa were obtained through the image database AntWeb [11] with specimen numbers noted in Data S1.

METHOD DETAILS

Phylogenetic dataset

A recent phylogenetic analysis of Cretaceous and modern ants indicated that hell ants are a monophyletic stem-group [3, 61]. However, at the time of this analysis, only three haidomyrmecine genera were known. We performed a series of expanded phylogenetic analyses under alternate optimality criteria and analytical parameters to assess 1) the internal relationships of the haidomyrmecines as well as 2) the position of hell ants within Formicidae. We constructed a morphological matrix with 65 unordered, discrete characters: 37 were drafted from the matrix of Barden and Grimaldi [3] – indicated with an asterisk* in the character list in Methods S1 – which itself comprised novel characters as well as characters from Keller [62]. Some haidomyrmecine taxa are known only from alates or workers. To reduce the impact of caste-specific morphological variation biasing the matrix construction and phylogenetic inference, we did not add any additional caste-specific characters. Taxa with unknown worker castes were coded as missing for worker-specific characters. Because some genera are only known from alate or dealate taxa, which can exhibit significantly different thoracic sculpturing, additional characters were selected primarily from the head and metasoma. Features from these areas vary less significantly among reproductive castes in known congeneric stem ant morphotypes. Eight of the newly added characters included inapplicable states based on contingent character systems (e.g. taxa without any horns were coded as inapplicable for characters representing horn-related states). Characters were coded for a total of 46 terminals: four outgroup taxa, 24 crown ants, and 18 stem ants (Table S1). Nine of the stem ant terminals

are within the Haidomyrmecinae. One of the crown ants, *Kyromyrma neffi*, is a fossil species included to assess the impact of incomplete data. All haidomyrmecine genera are monotypic, with the exception of *Haidomyrmex* and *Linguamyrmex*, which includes *H. scimitarus*, *H. zigrasi*, and the type species, *H. cerberus* and *L. brevicornis*, *L. rhinocerus*, and the type species *L. vladi*, respectively. Coding for *Haidomyrmex* and *Linguamyrmex* was based on chimeric scoring for all congeners, which were not found to be distinct in the context of characters selected here. The matrix included 2.8% missing states and 12.7% inapplicable states. Fossil taxa ranged between 0% missing data in cases where several specimens are known such as species of *Gerontoformica* to 21.5% with *Myanmyrma gracilis* known from a single fragmentary specimen.

Morphometric dataset

We compiled a dataset of clypeal and mandibular dimensions for 112 living and fossil ant species by taking measurements of imaged specimens from AntWeb [11] and fossil specimens (Data S1). Our measurements included:

Head length (HL) – length from the vertex to the anterior margin of the head capsule at or above the oral opening in lateral view.

Head depth (HD) – maximum depth of of the head in lateral view, comprising the frons or vertex at its dorsal-most and subgenal area at its ventral-most, excluding any clypeal horn in haidomyrmecines.

Clypeal length (CL) – length of the clypeus in lateral view from the anterior-most expanse of the clypeus to the posterior-most expansion of the clypeus (the posterior-most region may correspond to the epistomal sulcus or the subgenal sulcus, depending on the taxon). In cases where the epistomal sulcus is not visible from a lateral view, the posterior margin of the clypeus was approximated by noting the relative position of the sulcus to the antennal sockets in a frontal view, then measuring to this position.

Clypeal depth (CD) – maximum depth of the clypeus in lateral view from just above the mandibular insertion at its lowest to the maximum elevational height, taken perpendicular to CL.

Mandible length (ML) – Lateral length of mandible from insertion to apex.

Mandible height (MH) – Maximal height of mandible taken in lateral view from ventral-most to dorsal-most margins or teeth.

Our taxonomic sampling includes representatives of all 17 extant subfamilies (67 genera) and each known extant trap-jaw genus. We also sampled multiple congeners for lineages with highly specialized mandibles including *Dorylus*, *Harpegnathos*, *Mystrium*, and *Protalaridris.* Moreover, we sampled congeners from three trap-jaw genera with known internal phylogenetic relationships: *Anochetus*, *Odontomachus*, and *Strumigenys*. We took measurements for all taxa included in our morphology-based phylogenetic reconstruction (noted with * in Data S1), except for *Brownimecia*, *Haidomyrmodes*, *Myanmyrma*, and *Sphecomyrma* due to poor preservation. In the event that we could not locate suitable images or specimens, we substituted species included in the phylogeny for congeners for which we could collect accurate measurements (noted with ** in Data S1). To evaluate the relationship between traits in haidomyrmecines and extant ants, we created three size-scaled metrics of clypeus and mandible development:

Area – (Trait Length x Trait Height/Depth) / (Head Length x Head Depth)

Depth/Height – Trait Height/Depth / Head Length
Length – Trait Length / Head Length

Three-dimensional reconstructions

Models were constructed and rendered in Blender v2.79 (Blender Foundation, Amsterdam, Netherlands) by Oliver Budd, Jackson Fordham, and Victor Nzegwu, led by P.B. and Martina Decker at the New Jersey Institute of Technology (NIJT). To provide an initial foundation for digital sculpting, photomicrographs and a CT scan of *Haidomyrmex scimitarus* specimen AMNH BuFB80 were imported into Blender for side-by side comparison. The head morphology of *Haidomyrmodes* [2] and *Haidoterminus* [18] are largely similar to *Haidomyrmex*; these taxa were not modeled.

QUANTIFICATION AND STATISTICAL ANALYSIS

Phylogenetic analyses

The matrix was optimized under both parsimony and Bayesian inference (BI). Parsimony optimization included equal (EW) and implied weighting (IW). We ran tree searches agnostically without any topological constraints, and with the crown ant topology constrained to the results of the latest large-scale molecular phylogenetic hypothesis [51]. Morphological phylogenies have been in significant disagreement with molecular-based hypothesis, so this topological constraint was included to assess the sensitivity of our results to changing character polarity. Our phylogenetic assessment therefore included a total of six searches: EW Parsimony, IW Parsimony, and Bayesian inference each with and without a topological constraint (EWC, IWC, BIC, EWUC, IWUC, BIUC).

Trees were generated under a parsimony framework in TNT v1.5 (equal and implied weights) [63, 64]. All parsimony optimizations utilized the ‘xmult’ command with tree-drifting, ratchetting, and sectorial searches until the lowest score tree was identified one hundred times independently. Tree support was assessed with 1000 bootstrap pseudoreplicates. Topological constraints were employed with the “Force” command. Our unconstrained EW search returned 160 most parsimonious trees of 212 steps with a consistency index (CI) of 0.33 and retention index (RI) of 0.66; the constrained topology EW search resulted in four most parsimonious trees of 242 steps (CI: 0.32, RI: 0.65). Implied weights parsimony reconstructions were performed with the ‘xpiwe’ command with a default k-value of 3 [65]. The implied weights phylogeny was more resolved and supported (Fig. S1A) in both the unconstrained (CI: 0.37, RI: 0.77) and constrained (CI: 0.32, RI: 0.66) searches.

Bayesian inference was performed in MrBayes v3.2.7a [66]. We excluded character 13, antennal segment number, from Bayesian searches as it comprises a large number of character states. We specified variable coding with a gamma rate distribution i.e. under a Mkv + gamma model [67]. Searches were run for ten million generations with four chains under default parameters of three heated and one cold. We removed 25% of sampled trees as burn-in. Topology was fixed with the “constraint” command for the restricted topology search. We assessed convergence for searches by ensuring that the average standard deviation of split

frequencies was less than 0.01, potential scale reduction factors were equal to ~1, and estimated sample size (ESS) exceeded 200. ESS was assessed in Tracer v1.7.1 [68]. Because fossil branches do not terminate in the present, we performed phylogenetic estimation with tip-dating to generate more accurate branch lengths used in phylogenetic comparative methods. Tip dating allows for fossil terminals to calibrate divergence date estimates, which provides temporally informed branch length estimates for fossils [69, 70]. Using the same morphological matrix as in our BI phylogenetic analyses, we generated a phylogeny under a fossilized birth–death model in MrBayes [71]. We constrained monophyly according to the results of our BIC analysis and calibrated the phylogeny through Cretaceous fossil terminal dates. As in our BIC reconstruction, we applied a variable Mk + gamma model for a single morphological partition. We applied a clock-constrained fossilized birth-death model with the flat and fairly agnostic priors of Matzke and Wright [72] for our gamma distribution, clock rate, and birth-death (igrvarpr=uniform(0.0001, 200); clockratepr = normal(0.0025,0.1); speciationpr = uniform(0,10) ; extinctionpr, fossilizationpr = beta(1,1)). Our search was run for ten million generations with default chain and temperature settings. We again discarded 25% of sampled trees as burn in and assessed convergence as our BIC and BIUC runs. Our results (Fig. S1C) are not meant to provide divergence date alternatives to those derived from molecular-based phylogenetics, but rather are an attempt to generate another topological hypothesis that incorporates fossil age to assess the impact on comparative methods.

Morphospace analyses

To assess the comparative morphospace of hell ants, other stem-ants, crown ants, and non-ant aculeate outgroup taxa, we performed a series of principal coordinate analyses (PCo) and principal component analyses (PCA). Morphospace plots were generated from phylogenetic character matrices used in phylogenetic reconstruction, as in other analyses of morphospace of extinct taxa [73]. However, because inapplicable states can generate artificial positions in morphospace [74], morphological matrices were pruned of characters with inapplicable (-) states for any terminal. In addition, to ensure that morphospaces were not primarily driven by missing data for fossil taxa or anatomical partitioning, we generated three morphospaces: data were subsampled into 1) cephalic-only (Fig. 2A) and 2) all-character datasets (Fig. S1B) for PCo analyses and 3) a matrix with no missing data for PCA analysis (Fig. S1B). We generated euclidean distance matrices in R and PCo analyses with the ‘pco’ command in the LabDSV library [75]. The outgroup taxon *Heterogyna* possessed a great deal of inapplicable states, and so was removed from PCo and PCA analyses to include more characters. The taxa *Brownimecia clavata*, *Haidomyrmodes mammuthus*, and *Myanmyrma gracilis* contain the greatest number of missing states. These taxa were excluded from the PCA analysis to allow for greater character sampling as PCA analyses cannot incorporate missing data.

Phylogenetic comparative methods

To assess the relationship between clypeus and mandible, we performed a series of linear regressions on phylogenetic independent contrast scores informed from different taxonomic sampling treatments. Our taxonomic sampling reflected the match between our phenotypic dataset and available phylogenetic hypotheses. Treatments are outlined in Table S2. We performed two extant “formicidae-wide” analyses: one incorporating our dated morphological

phylogeny (pruned to 24 matching terminals) and one incorporating the Bayesian genus-tree of Blanchard & Moreau [76] (pruned to 61 matching terminals). We also generated contrast scores for five subfamily-specific treatments: Haidomyrmecinae (our dated morphological phylogeny pruned to 8 matching terminals), Dorylinae (Blanchard & Moreau [76] pruned to 11 matching terminals), Formicinae (the UCE-100 best loci phylogeny of Blaimer et al. [77] pruned to 9 matching terminals), Mymicinae (Blanchard & Moreau [76] pruned to 15 matching terminals), and Ponerinae (Blanchard & Moreau [76] pruned to 10 matching terminals) as well as three genus-specific treatments, each pruned to nine terminals: *Anochetus* [78], *Odontomachus* [79], and *Strumigenys* [80]. To account for mismatch of species between phylogenies and phenotypic data, we performed analyses at the genus level and did not included multiple congeners in subfamily-specific and formicidae-wide datasets. Generic representatives we included in the Blaimer et al. [77] and Blanchard & Moreau [76] analyses are noted in Data S1 under the column "Data Species". Contrast scores were generated for all metrics of clypeal and mandibular expansion with the "pic" command in the R package ape [81]: Area, Depth/Height, and Length. We then fit linear models to contrast scores in R using the "lm" command. Resulting summary statistics are presented in Table S2 as well as Figures 2 and S2. Across all metrics, hell ants exhibit increased slopes and R-squared values for the linear relationship between clypeus and mandibles relative to extant ant treatments. Reduced Extant-only and Ponerinae-only analyses of clypeal depth and mandible height as well as our *Odontomachus*-only clypeal area and mandibular area analysis recover significant linear relationships, although with reduced slopes and fit than in the case of hell ants. We presented our area-metric in the main-text as it includes both individual depth/height and length measurement data.

We also assessed integration between clypeal and mandibular dimensions in a Bayesian framework with the R package ratematrix [82], which can be used to assess correlation between traits across a phylogeny. We pruned our dated molecular phylogeny to terminals for which we had phenotypic data and labeled all tips as either "hell" mandibular syndrome (dorsally expanded to meet clypeal extensions as in all hell ants) for haidomyrmecines and "typ" mandibular syndrome (typical mandibular development reflected in taxa with horizontal mouthpart articulation, i.e. all non-hell ants) for all other ant taxa. Our tip labeling reflected two reciprocally monophyletic groups of "hell" or "typ" taxa. We then generated 100 simulated trees with stochastic character mapping for the two mandibular syndromes with the 'make.simmap' command in phytools [83]. This sample of trees and our phenotypic data (clypeal and mandibular area, height/depth, and length) were used in two MCMC chain runs employed with 'ratematrixMCMC', each spanning five million generations. We discarded 25% of resulting samples as burn in and assessed convergence with the 'checkConvergence' command. We then merged the two chain samples and extracted the posterior distribution and degree of overlap for evolutionary correlation with the 'extractCorrelation' and 'testRatematrix' commands, respectively. We also repeated this process after converting our dated tree to ultrametric with the 'extend' method in phytools to assess any impact in differing branch lengths. Our results (Fig. S2D) recover hell ants as consistently exhibiting higher degrees of evolutionary correlation across clypeal and mandibular area, height/depth, and length in both ultrametric and non-ultrametric treatments. We identify a lower degree of overlap in area and height dimensions for non-ultrametric (area: 10.2%; height/depth: 17.1%; length: 48.1%) and ultrametric (area: 24.5%;

height/depth: 30.1%; length: 46.3%) treatments, mirroring the results of our PIC analyses but demonstrating a less extreme difference between hell ants and crown ants with this methodology.

References

1. Dlussky, G.M. (1996). Ants (Hymenoptera: Formicidae) from Burmese amber. Paleontol. J. *30*, 449–454.
2. Perrichot, V., Nel, A., Néraudeau, D., Lacau, S., and Guyot, T. (2008). New fossil ants in French Cretaceous amber (Hymenoptera: Formicidae). Naturwissenschaften *95*, 91–97.
3. Barden, P., and Grimaldi, D.A. (2016). Adaptive radiation in socially advanced stem-group ants from the Cretaceous. Curr. Biol. *26*, 515–521.
4. Perrichot, V., Wang, B., and Engel, M. S. (2016). Extreme morphogenesis and ecological specialization among Cretaceous basal ants. Curr. Biol. *26*, 1468–1472.
5. Barden, P, Herhold, H.W., and Grimaldi, D.A. (2017). A new genus of hell ants from the Cretaceous (Hymenoptera: Formicidae: Haidomyrmecini) with a novel head structure. Syst. Entomol. *42*, 837–846.
6. Perrichot, V., Wang, B., and Barden, P. (2020). New remarkable hell ants (Formicidae: Haidomyrmecinae stat. nov.) from Cretaceous Burmese amber. Cretaceous Res. *109*, 104381.
7. Bolton, B. (2020). An online catalog of the ants of the world. Available from http://antcat.org.
8. Hölldobler, B., and Wilson, E.O. (1990). The ants (Cambridge: Harvard University Press).
9. Oster, G.F., and Wilson, E.O. (1978) Caste and Ecology in the Social Insects (Princeton: Princeton University Press).
10. Beldade, P., Mateus, A.R.A., and Keller, R.A. (2011). Evolution and molecular mechanisms of adaptive developmental plasticity. Mol. Ecol. *20*, 1347–1363.
11. AntWeb. (2020). Version 8.38.1. California Academy of Science. Available from https://www.antweb.org.
12. Wilson, E.O., Carpenter, F.M., and Brown, W.L. (1967). The first Mesozoic ants. Science *157*, 1038–1040.
13. Wilson, E.O. (1985). Ants from the Cretaceous and Eocene amber of North America. Psyche *92*, 205–216.
14. Engel, M.S., and Grimaldi, D.A. (2005). Primitive new ants in Cretaceous amber from Myanmar, New Jersey, and Canada (Hymenoptera: Formicidae). Am. Mus. Novit. *3485*, 1–24.
15. Barden, P., and Grimaldi, D.A. (2013). A new genus of highly specialized ants in Cretaceous Burmese amber (Hymenoptera: Formicidae). Zootaxa *3681*, 405–412.
16. LaPolla, J.S., Dlussky, G.M., and Perrichot, V. (2013). Ants and the Fossil Record. Annu. Rev. Entomol. *58*, 609–630.
17. Perrichot, V. (2014). A new species of the Cretaceous ant *Zigrasimecia* based on the worker caste reveals placement of the genus in the Sphecomyrminae (Hymenoptera: Formicidae). Myrmecol. News *19*, 165–169.

18. McKellar, R.C., Glasier, J., and Engel, M.S. (2013). A new trap-jawed ant (Hymenoptera: Formicidae: Haidomyrmecini) from Canadian Late Cretaceous amber. *Can. Entomol. 145*, 454–465.
19. Miao, Z., and Wang, M. (2019). A new species of hell ants (Hymenoptera: Formicidae: Haidomyrmecini) from the Cretaceous Burmese amber. J. Guangxi Normal Univ. *37*, 139–142.
20. Simpson, G.G. (1944) Tempo and mode in evolution. (New York: Columbia University Press).
21. Valentine, J.W. (1980). Determinants of diversity in higher taxonomic categories. Paleobiology *6*, 444–450.
22. Foote, M. (1997). The evolution of morphological diversity. Annu. Rev. Ecol. Syst. *28*, 129–152.
23. Gavrilets, S., and Losos, J.B. (2009). Adaptive radiation: contrasting theory with data. Science *323*, 732–737.
24. Slater, G.J., Price, S.A., Santini, F., and Alfaro, M.E. (2010). Diversity versus disparity and the radiation of modern cetaceans. Proc. R. Soc. B. *277*, 3097–3104.
25. Pie, M.R., and Traniello, J.F.A. (2007). Morphological evolution in a hyperdiverse clade: the ant genus *Pheidole*. J. Zool. *271*, 99–109.
26. Sarnat, E. M., Friedman, N. R., Fischer, G., Lecrocq-Bennet, B., and Economo, E. P. (2017). Rise of the spiny ants: diversification, ecology and function of extreme traits in the hyperdiverse genus *Pheidole* (Hymenoptera: Formicidae). Biol. J. Linn. Soc. *122*, 514–538.
27. Wilson, E.O., and Hölldobler, B. (1986). Ecology and behavior of the neotropical cryptobiotic ant *Basiceros manni* (Hymenoptera: Formicidae: Basicerotini). Insect. Soc. *33*, 70–84.
28. Gnatzy, W., and Maschwitz, U. (2006). Pedestal hairs of the ant *Echinopla melanarctos* (Hymenoptera, Formicidae): morphology and functional aspects. Zoomorphology *125*, 57–68.
29. Dornhaus, A., and Powell, S. (2010). Foraging and defence strategies. In Ant ecology, Lach, L., Parr, C. L. & Abott, K. L., eds. (New York: Oxford University Press), pp. 210–230.
30. Gotwald Jr., W.H. (1969). Comparative morphological studies of the ants, with particular reference to the mouthparts (Hymenoptera: Formicidae). Cornell Univ. Agric. Exp. Station Mem. *408*, 1–150.
31. Schumann, R.D. 1992. Raiding behavior of the dulotic ant *Chalepoxenus muellerianus* (Finzi) in the field (Hymenoptera: Formicidae, Myrmicinae). Insect. Soc. *39*, 325–333.
32. Brandão, C.R.F., Diniz, J.L.M., and Tomotake, E.M. (1991). *Thaumatomyrmex* strips millipedes for prey: a novel predatory behaviour in ants, and the first case of sympatry in the genus (Hymenoptera: Formicidae). Insect. Soc. *38*, 335–344.
33. Paul, J. (2001). Mandible movements in ants. Comp. Biochem. Phys. A. *131*, 7–20.
34. Barden, P., and Grimaldi, D.A. (2012). Rediscovery of the bizarre Cretaceous ant *Haidomyrmex* Dlussky (Hymenoptera: Formicidae), with two new species. Am. Mus. Novit. *3755*, 1–16.

35. Shi, G., Grimaldi, D.A., Harlow, G.E., Wang, J., Wang, J., Yang, M., Lei, W., Li, Q., and Li, X. (2012). Age constraint on Burmese amber based on U–Pb dating of zircons. Cretaceous Res. *37*, 155–163.
36. Bai, M., Beutel, R.G., Klass, K.D., Zhang, W., Yang, X., and Wipfler, B. (2016). †Alienoptera—A new insect order in the roach–mantodean twilight zone. Gondwana Res. *39*, 317–326.
37. Bai, M., Beutel, R.G., Zhang, W., Wang, S., Hörnig, M., Gröhn, C., Yan, E., Yang, X., and Wipfler, B. (2018). A new Cretaceous insect with a unique cephalo-thoracic scissor device. Curr. Biol. *28*, 438–443.
38. Kočárek, P. (2018). The cephalo-thoracic apparatus of Caputoraptor elegans may have been used to squeeze prey. Curr. Biol. *28*, R824-R825.
39. Richter, A., Keller, R.A., Rosumek, F.B., Economo, E.P., Garcia, F.H., and Beutel, R.G. (2019). The cephalic anatomy of workers of the ant species *Wasmannia affinis* (Formicidae, Hymenoptera, Insecta) and its evolutionary implications. Arthropod Struct. & Dev. *49*, 26–49.
40. Moffett, M.W. (1986). Trap-jaw predation and other observations on two species of *Myrmoteras* (Hymenoptera: Formicidae). Insect. Soc. *33*, 85–99.
41. Snodgrass, R.E. (1935). Principles of insect morphology (Ithaca: Cornell University Press).
42. Bolton, B. (2003). Synopsis and classification of Formicidae. Mem. Am. Entomol. Inst. *71*, 1–370.
43. Larabee, F.J., and Suarez, A.V. (2014). The evolution and functional morphology of trap-jaw ants (Hymenoptera: Formicidae). Myrmecol. News *19*, 25–36.
44. Gronenberg, W. (1995). The fast mandible strike in the trap-jaw ant *Odontomachus*. J. Comp. Physiol. A. *176*, 399–408.
45. Bolton, B. (1999). Ant genera of the tribe Dacetonini (Hymenoptera: Formicidae). J. Nat. Hist. *33*, 1639–1689.
46. Patek, S.N., Baio, J.E., Fisher, B.L., and Suarez, A.V. (2006). Multifunctionality and mechanical origins: ballistic jaw propulsion in trap-jaw ants. Proc. Natl. Acad. Sci. USA *103*, 12787–12792.
47. Ehmer, B., and Hölldobler, B. (1995). Foraging behavior of *Odontomachus bauri* on Barro Colorado island, Panama. Psyche *102*, 215–224.
48. Brady, S.G., Schultz, T.R., Fisher, B.L., and Ward, P.S. (2006). Evaluating alternative hypotheses for the early evolution and diversification of ants. Proc. Natl. Acad. Sci. USA *103*, 18172–18177.
49. Moreau, C.S., Bell, C.D., Vila, R., Archibald, S.B., and Pierce, N.E. (2006). Phylogeny of the ants: diversification in the age of angiosperms. Science *312*, 101–104.
50. Moreau, C.S., and Bell, C.D. (2013). Testing the museum versus cradle tropical biological diversity hypothesis: phylogeny, diversification, and ancestral biogeographic range evolution of the ants. Evolution *67*, 2240–2257.
51. Borowiec, M.L., Rabeling, C., Brady, S.G., Fisher, B.L., Schultz, T.R., and Ward, P.S. (2019). Compositional heterogeneity and outgroup choice influence the internal phylogeny of the ants. Mol. Phylogenet. and Evol. *134*, 111–121.

52. Economo, E.P., Narula, N., Friedman, N.R., Weiser, M.D., and Guénard, B. (2018). Macroecology and macroevolution of the latitudinal diversity gradient in ants. Nat. Comm. *9*, 1778.
53. Pie, M.R., and Tschá, M.K. (2009). The macroevolutionary dynamics of ant diversification. Evolution *63*, 3023–3030.
54. Hughes, M., Gerber, S., and Wills, M.A. (2013). Clades reach highest morphological disparity early in their evolution. Proc. Natl. Acad. Sci. USA *110*, 13875–13879.
55. Harmon, L.J., Losos, J.B., Davies, J.T., Gillespie, R.G., Gittleman, J.L., Jennings, B.W., Kozak, K.H., McPeek, M.A., Moreno-Roark, F., Near, T.J. and Purvis, A. (2010). Early bursts of body size and shape evolution are rare in comparative data. Evolution *64*, 2385-–2396.
56. Hopkins, M.J., and Smith, A.B. (2015). Dynamic evolutionary change in post-Paleozoic echinoids and the importance of scale when interpreting changes in rates of evolution. Proc. Natl. Acad. Sci. USA *112*, 3758–3763.
57. Böving, A.G., and Craighead, F.C. (1931) An illustrated synopsis of the principal larval forms of the order Coleoptera (Brooklyn: Brooklyn Entomological Society).
58. Friis, H., Bauer, T., and Betz, O. (2003). An insect larva with a 'pig-snout': structure and function of the nasale of *Hyphydrus ovatus* L. (1763) (Coleoptera: Dytiscidae). J. Zool. *261*, 5968.
59. Hayashi, M., and Ohba, S.Y. (2018). Mouth morphology of the diving beetle *Hyphydrus japonicus* (Dytiscidae: Hydroporinae) is specialized for predation on seed shrimps. Biol. J. Linn. Soc. *125*, 315–320.
60. Armbruster, W.S., Pélabon, C., Bolstad, G.H., and Hansen, T.F. (2014). Integrated phenotypes: understanding trait covariation in plants and animals. Philos. T. R. Soc. B. *369*, 20130245.
61. Barden, P. (2017). Fossil ants (Hymenoptera: Formicidae): ancient diversity and the rise of modern lineages. Myrmecol. News *24*, 1–30.
62. Keller, R.A. (2011). A phylogenetic analysis of ant morphology (Hymenoptera: Formicidae) with special reference to the poneromorph subfamilies. B. Am. Mus. Nat. Hist. *355*, 1–90.
63. Goloboff, P.A., and Catalano, S.A. (2016). TNT version 1.5, including a full implementation of phylogenetic morphometrics. Cladistics *32*, 221–238.
64. Goloboff, P.A. (1993). Estimating character weights during tree search. Cladistics *9*, 83–91.
65. Goloboff, P.A. (2014). Extended implied weighting. Cladistics *30*, 260–272.
66. Ronquist, F., Teslenko, M., Van Der Mark, P., Ayres, D.L., Darling, A., Höhna, S., Larget, B., Liu, L., Suchard, M.A., and Huelsenbeck, J.P. (2012). MrBayes 3.2: efficient Bayesian phylogenetic inference and model choice across a large model space. Syst. Biol. *61*, 539–542.
67. Lewis, P.O. (2001). A likelihood approach to estimating phylogeny from discrete morphological character data. Syst. Biol. *50*, 913–925.
68. Rambaut, A., Drummond, A.J., Xie, D., Baele, G., and Suchard, M.A. (2018). Posterior summarization in Bayesian phylogenetics using Tracer 1.7. Syst. Biol. *67*, 901–904.

69. Ware, J.L., Grimaldi, D.A., and Engel, M.S. (2010). The effects of fossil placement and calibration on divergence times and rates: an example from the termites (Insecta: Isoptera). Arthropod Struct. & Dev. *39*, 204–219.
70. Ronquist, F., Klopfstein, S., Vilhelmsen, L., Schulmeister, S., Murray, D.L., and Rasnitsyn, A.P. (2012). A total-evidence approach to dating with fossils, applied to the early radiation of the Hymenoptera. Syst. Biol. *61*, 973–999.
71. Zhang, C., Stadler, T., Klopfstein, S., Heath, T.A., and Ronquist, F. (2015). Total-evidence dating under the fossilized birth–death process. Syst. Biol. *65*, 228249.
72. Matzke, N.J., and Wright, A. (2016). Inferring node dates from tip dates in fossil Canidae: the importance of tree priors. *Biol. Letters 12*, 20160328.
73. Brusatte, S.L. Benton, M.J., Ruta, M., and Lloyd, G.T. (2008). Superiority, competition, and opportunism in the evolutionary radiation of dinosaurs. Science *321*, 1485–1488.
74. Gerber, S. (2019). Use and misuse of discrete character data for morphospace and disparity analyses. Palaeontology *62*, 305–319.
75. Roberts, D.W. (2007). LabDSV: Ordination and multivariate analysis for ecology. R package version, 1.
76. Blanchard, B.D., and Moreau, C.S. (2017). Defensive traits exhibit an evolutionary trade-off and drive diversification in ants. Evolution *71*, 315–328.
77. Blaimer, B.B., Brady, S.G., Schultz, T.R., Lloyd, M.W., Fisher, B.L., and Ward, P.S. (2015). Phylogenomic methods outperform traditional multi-locus approaches in resolving deep evolutionary history: a case study of formicine ants. BMC Evol. Biol. *15*, 271.
78. Larabee, F.J., Fisher, B.L., Schmidt, C.A., Matos-Maraví, P., Janda, M., and Suarez, A.V. (2016). Molecular phylogenetics and diversification of trap-jaw ants in the genera *Anochetus* and *Odontomachus* (Hymenoptera: Formicidae). Mol. Phylogenet. and Evol. 103, 143–154.
79. Matos-Maraví, P., Matzke, N.J., Larabee, F.J., Clouse, R.M., Wheeler, W.C., Sorger, D.M., Suarez, A.V., and Janda, M. (2018). Taxon cycle predictions supported by model-based inference in Indo-Pacific trap-jaw ants (Hymenoptera: Formicidae: *Odontomachus*). Mol. Ecol. *27*, 4090–4107.
80. Ward, P.S., Brady, S.G., Fisher, B.L., and Schultz, T.R. (2015). The evolution of myrmicine ants: phylogeny and biogeography of a hyperdiverse ant clade (Hymenoptera: Formicidae). Syst. Entomol. *40*, 61–81.
81. Paradis, E., Claude, J., and Strimmer, K. (2004). APE: analyses of phylogenetics and evolution in R language. Bioinformatics *20*, 289–290.
82. Caetano, D.S., and Harmon, L.J. (2017). ratematrix: An R package for studying evolutionary integration among several traits on phylogenetic trees. Methods. Ecol. Evol. *8*, 1920–1927.
83. Revell, L.J. (2012). phytools: an R package for phylogenetic comparative biology (and other things). Methods. Ecol. Evol. *3*, 217–223.

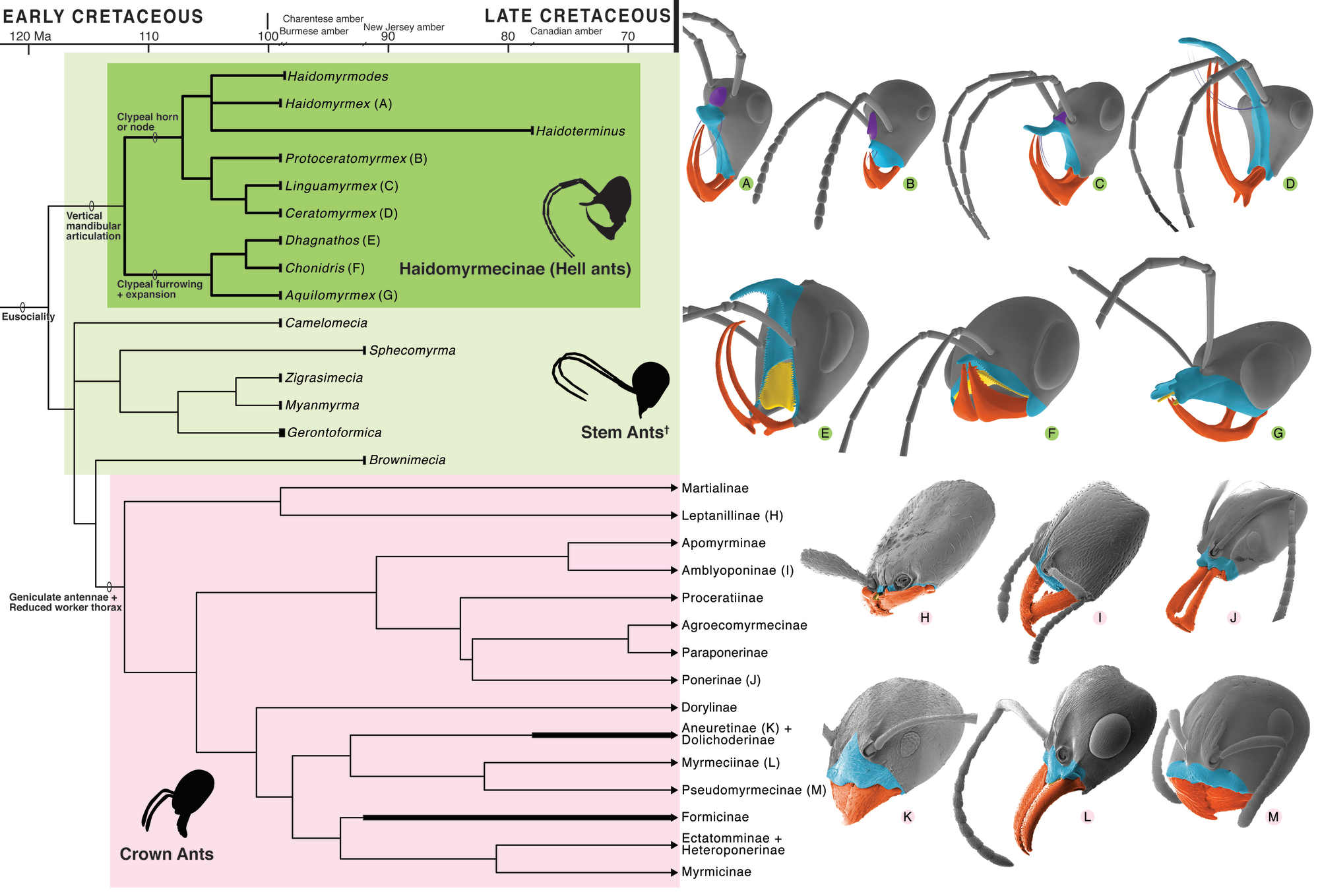
EARLY CRETACEOUS
LATE CRETACEOUS
120 Ma
110
100
90
80
70
Charentese amber
Burmese amber
New Jersey amber
Canadian amber
Haidomyrmodes
Haidomyrmex (A)
Haidoterminus
Protoceratomyrmex (B)
Linguamyrmex (C)
Ceratomyrmex (D)
Dhagnathos (E)
Chonidris (F)
Aquilomyrmex (G)
Clypeal horn or node
Vertical mandibular articulation
Clypeal furrowing + expansion
Haidomyrmecinae (Hell ants)
Eusociality
Camelomecia
Sphecomyrma
Zigrasimecia
Myanmyrma
Gerontoformica
Brownimecia
Stem Ants†
Geniculate antennae + Reduced worker thorax
Martialinae
Leptanillinae (H)
Apomyrminae
Amblyoponinae (I)
Proceratiinae
Agroecomyrmecinae
Paraponerinae
Ponerinae (J)
Dorylinae
Aneuretinae (K) + Dolichoderinae
Myrmeciinae (L)
Pseudomyrmecinae (M)
Formicinae
Ectatomminae + Heteroponerinae
Myrmicinae
Crown Ants
A
B
C
D
E
F
G
H
I
J
K
L
M

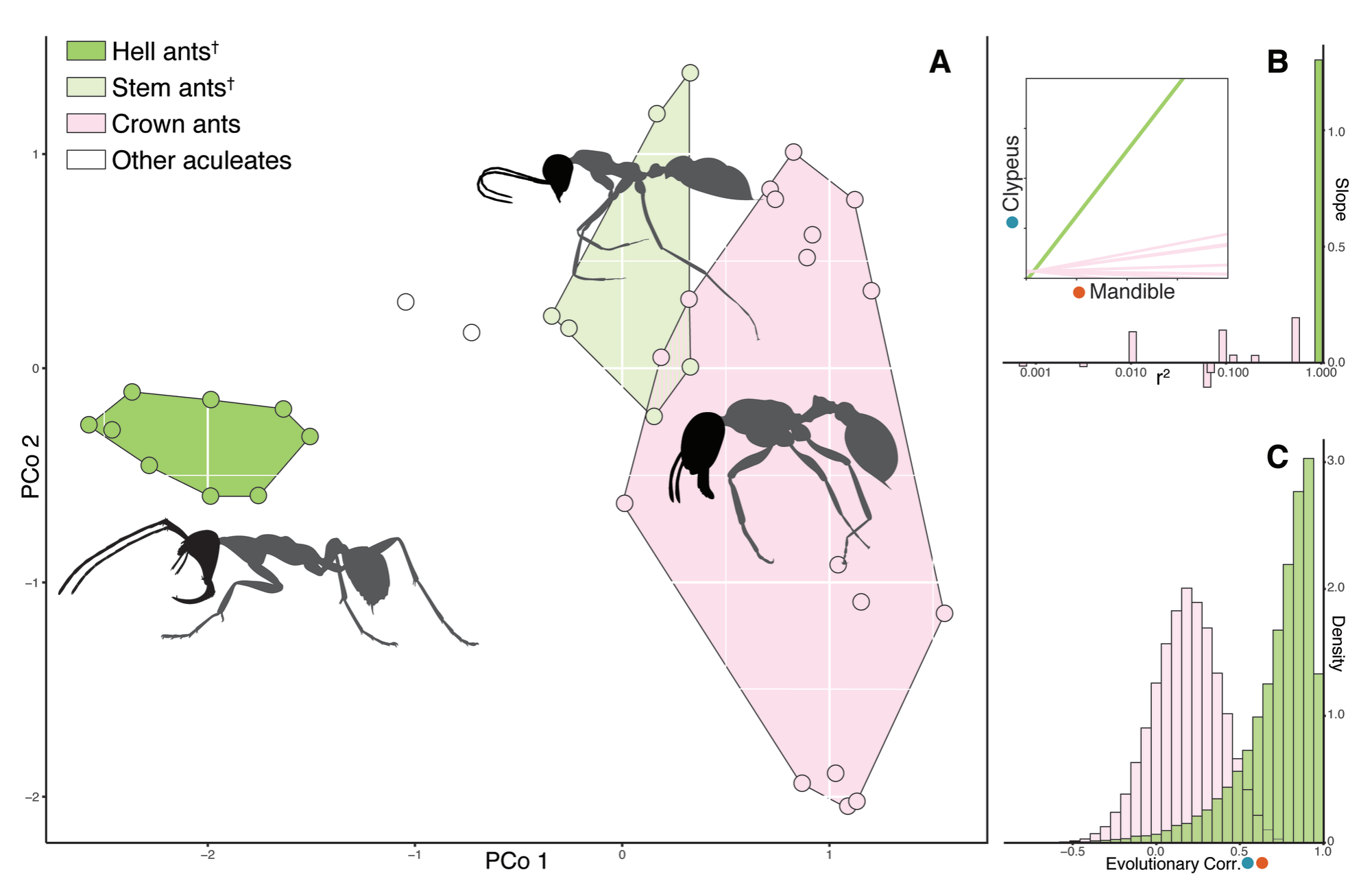
Hell ants†
Stem ants†
Crown ants
Other aculeates
A
B
C
PCo 1
PCo 2
Clypeus
Mandible
Slope
r²
Density
Evolutionary Corr.

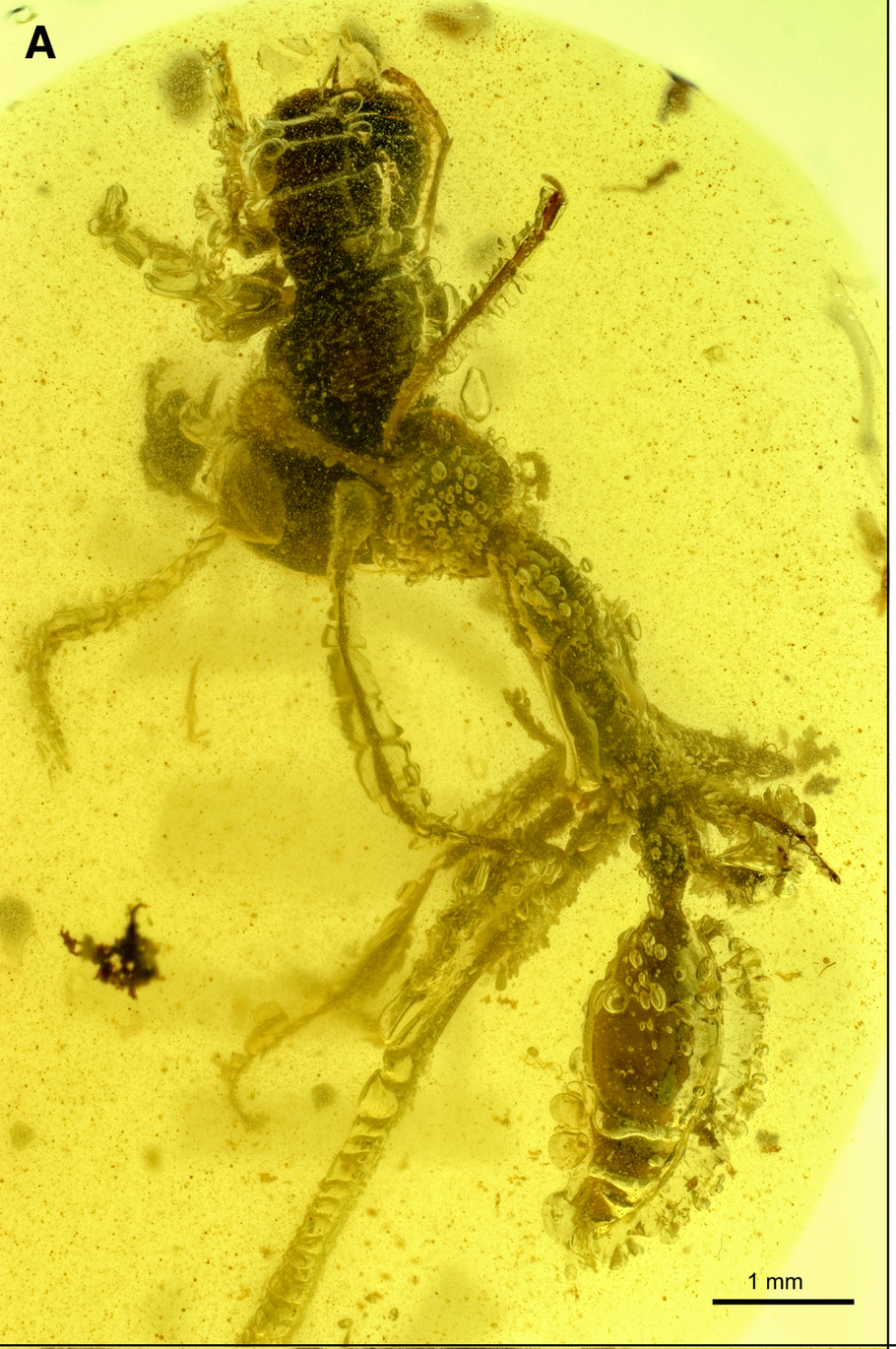
A
1 mm

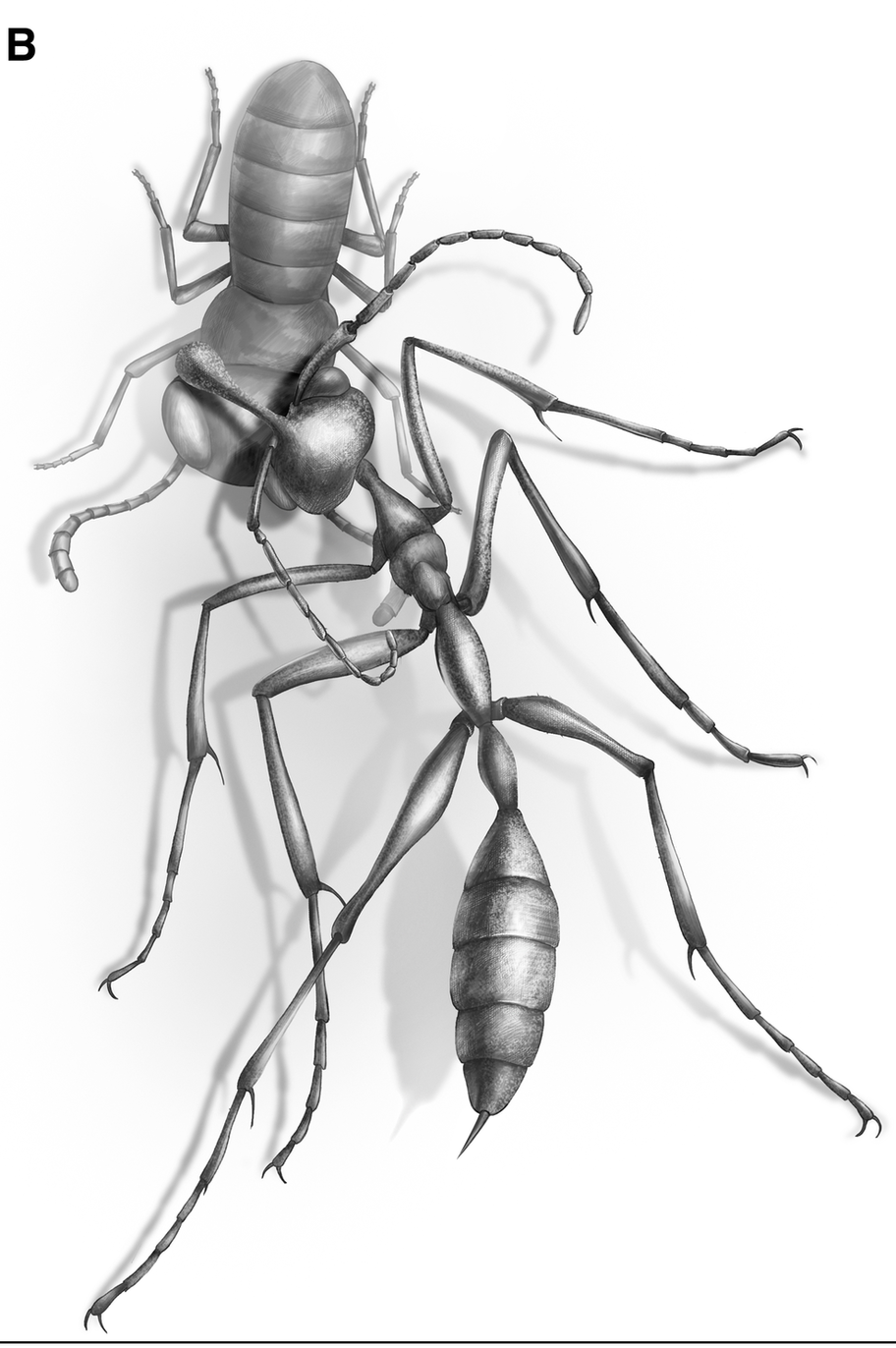
B

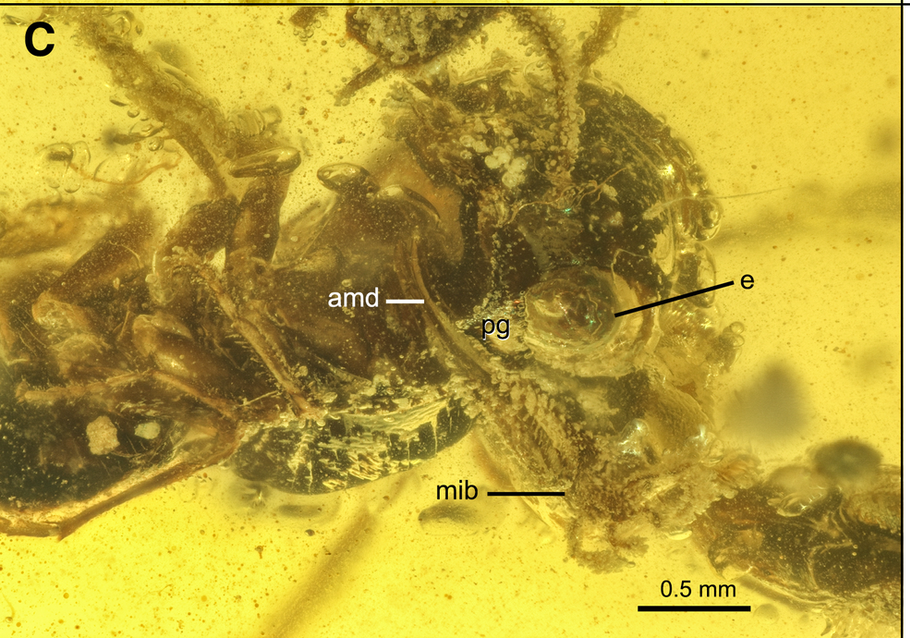
C
amd
pg
e
mib
0.5 mm

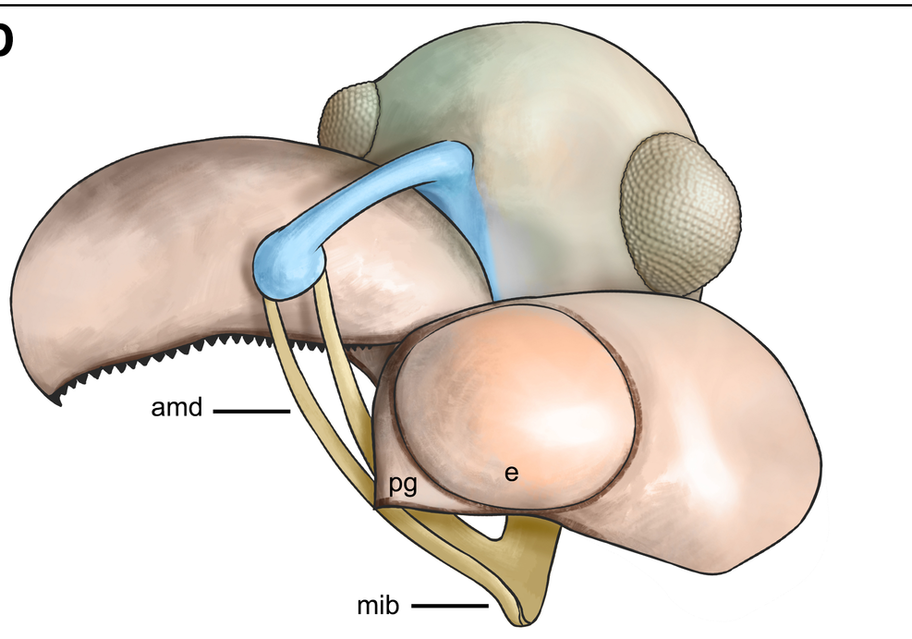
D
amd
pg
e
mib

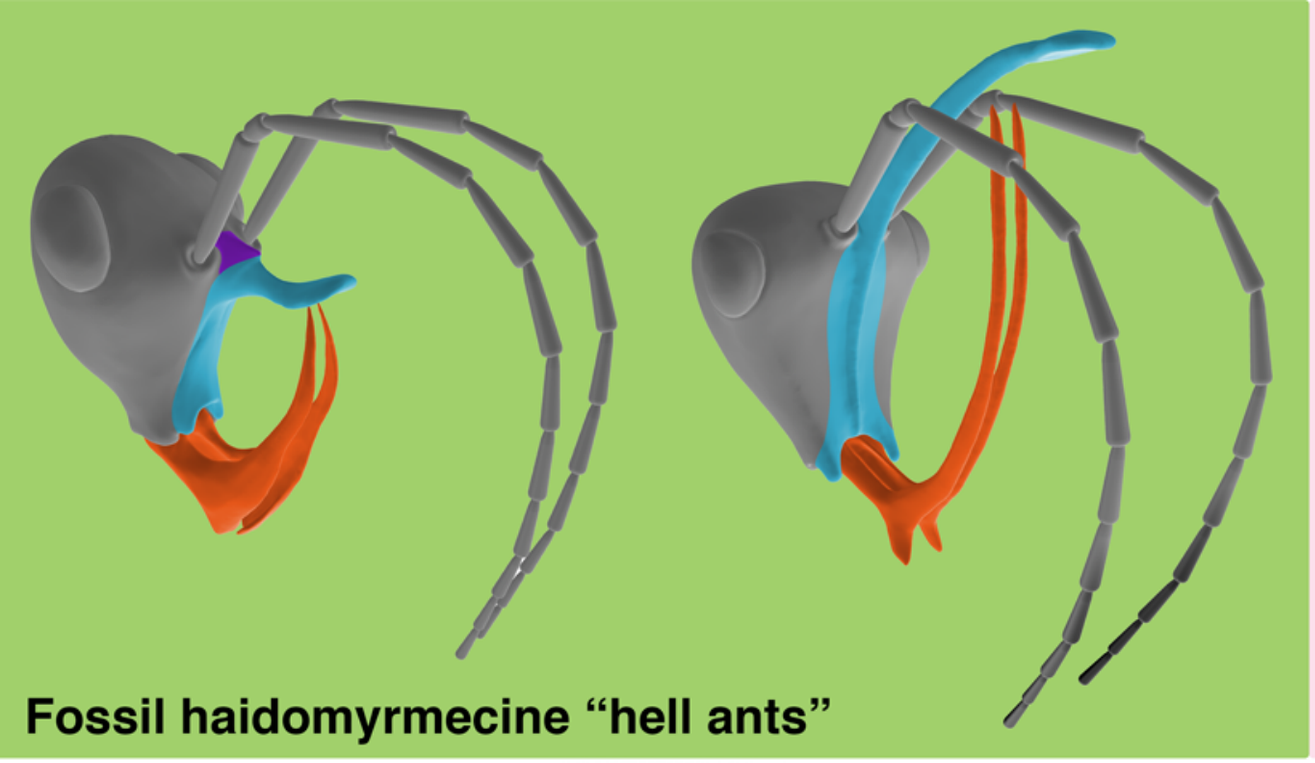

Fossil haidomyrmecine “hell ants”

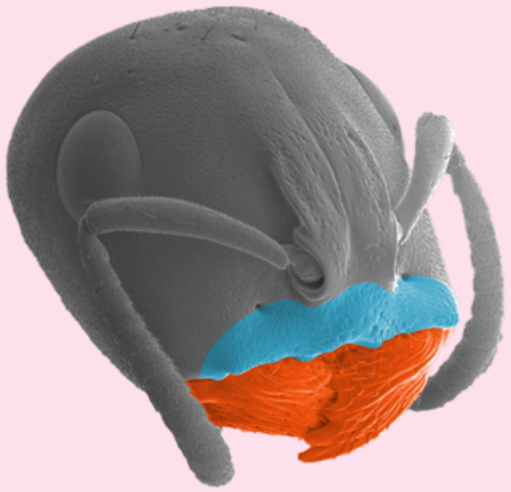

Extant ants

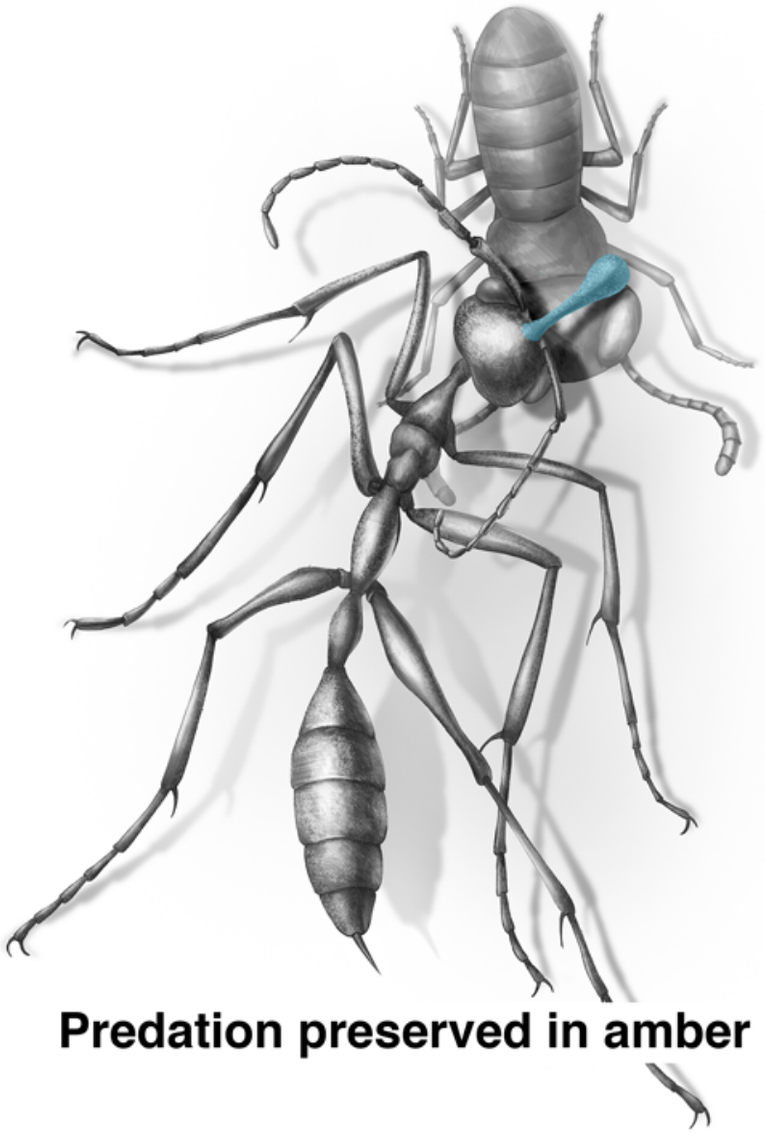

Predation preserved in amber

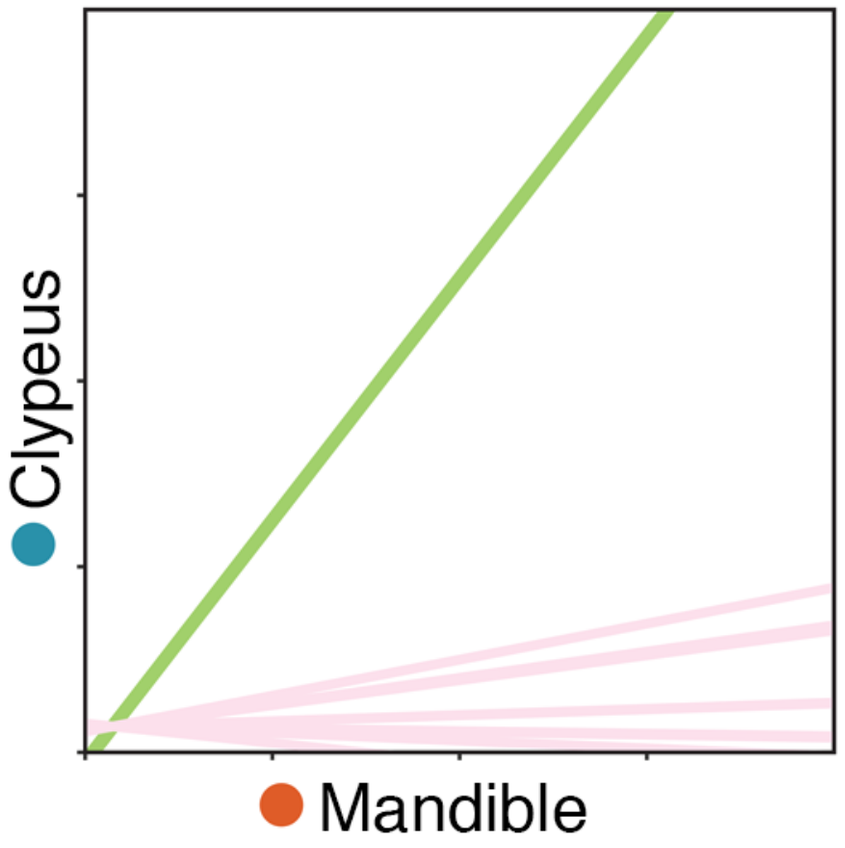

The head and mandibles of hell ants are uniquely integrated as a result of specialized prey capture